Numerical Evaluation of the Impulse Response of Multimode Optical Fibers

J. A. Arnaud*

A numerical technique based on ray optics is presented that provides the impulse response of multimode optical fibers having arbitrary smooth index profiles and arbitrary material dispersion. The variation of $dn/d\lambda_0$ as a function of n when the dopant concentration varies is obtained from Fleming[1] measurements on bulk samples. This technique is applied to germania-doped multimode fibers with power-law profiles and various values of $\Delta \equiv \Delta n/n$. Previous results[2] are shown to be invalid when $\Delta \gtrsim 0.005$. By successive approximations, optimum profiles that minimize the impulse response widths for quasi-monochromatic sources are found. For these optimum profiles, the quasi-monochromatic root-mean-square (rms) impulse response width is found to be of the order of 150 Δ^2nsec/km, in agreement with a recent analytical result.[3]

The transmission of information by means of optical pulses in glass fibers is increasingly promising. Losses as low as 0.5 dB/km at $\lambda_0 = 1.2$ μm have been reported.[4] These very low losses open the prospect of repeater spacings as large as 50 km. For large repeater spacings, a paramount problem is the broadening of the optical pulses, even at moderately low data rates. This is the problem we are addressing.

One key question in the design of optical fiber links—yet to be answered—is whether it is more economical to use (1) single-mode lasers, such as neodymium YAG lasers and single-mode fibers, (2) injection lasers and multimode fibers with moderate values of $\Delta \equiv \Delta n/n$, or (3)

* Bell Laboratories, Crawford Hill Laboratory, Holmdel, N.J.

Fiber and Integrated Optics, Volume 1, Number 1

surface light-emitting diodes (LEDs) and multimode fibers, preferably with large Δ at wavelengths of the order of 1.2 μm.* LEDs operating in that wavelength range have been reported.[5] A fourth alternative, which is in a sense intermediate to (1), (2), and (3), is to use edge-emitting LEDs and optical fibers that have a profile elongated in the plane of the LED junction.† In the present paper, we shall discuss only the problem of pulse broadening in multimode fibers. These fibers are presently easier to splice and cable than monomode fibers. (For a theoretical comparison of the microbending losses, see ref. 6.)

Numerical techniques for evaluating pulse broadening based on the Maxwell equations[7] are rigorous in principle, but very costly in terms of computing time. Numerical techniques based on ray optics (WKB approximation) are much more economical. They are accurate enough for multimode fibers that have smooth profiles. Irrespective of the basic equations used, it is essential to account for the fact that the ratio of the local phase and group velocities varies within the fiber cross section. This variation is called "inhomogeneous dispersion."[8,9] Because of inhomogeneous dispersion, the time of flight of pulses along a particular ray trajectory is not proportional to the optical length of the ray, and optical-length equalization does not ensure time-of-flight equalization. The practical importance of inhomogeneous dispersion in the design of graded-index multimode fibers was first pointed out in 1975.[2] The basic ray-optics equations that take inhomogeneous dispersion into account were given the year before.[11] It has also been shown[11] how these equations can be derived from wave optics, and how optimum profiles can be generated that take inhomogeneous dispersion into account.

Let us briefly review a few known analytical results and explain the reason for their inadequacy. One result[2] rests implicitly on the assumption that $ndn/d\lambda_0$ is proportional to n^2 as the dopant concentration varies. But as other recent measurements show,[1] this is usually not the

* Fibers with large Δ (e.g., with germania doping) are much less sensitive to microbending loss than fibers with small Δ, and the coupling efficiency to spatially incoherent sources, such as LEDs, is much better. However, for some dopants, it is not practical to raise (or lower) the index much with respect to that of pure silica. It can also be argued that if very low loss fibers can be fabricated, as now appears to be the case, one can afford to have relatively large coupling losses at the source. Therefore, the practical importance of large Δ fibers is difficult to assess at the moment.

† Fibers with elongated (e.g., elliptical) profiles may be useful in conjunction with edge-emitting LED sources and edge-receiving detectors, because the coherence of the field is preserved in one plane and the amount of dopant material used is minimized. Such profiles would also be less sensitive to microbends than round fibers if the Δ and the mechanical deformations were identical.

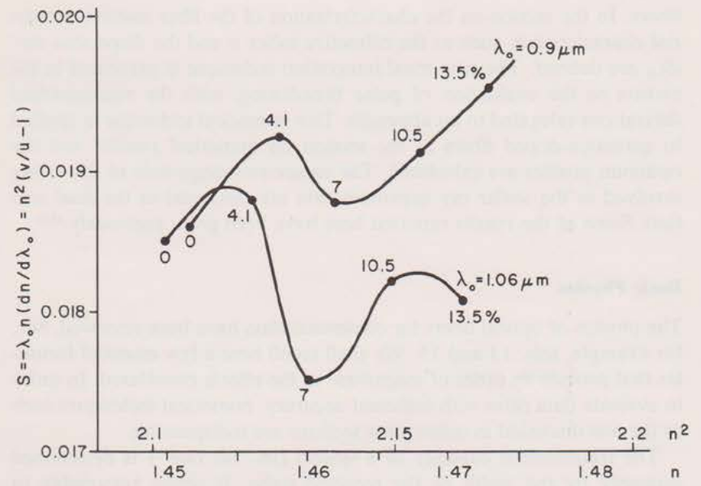

Fig. 1. Variation of $S = -\lambda_0 n(dn/d\lambda_0)$ as a function of n or n^2 for germania-doped fibers, at $\lambda_0 = 0.9$ and 1.06 μm from measurements[1] on bulk samples. The accuracy on S is about $\pm 1\%$. Note that these curves exhibit large departures from linearity.

case, except perhaps for fibers with very small $\Delta \equiv \Delta n/n$, typically $\Delta < 0.005$. (See Fig. 1.) A first-order perturbation method[12] can handle arbitrary variations of $ndn/d\lambda_0$ with n^2, but it is restricted to small departures of the index profile from a square-law profile. When the class of materials used in the fiber exhibits large variations of $dn/d\lambda_0$, the optimum profiles are far from square-law profiles and the first-order perturbation method[12] may not be accurate enough. Closed-form second-order perturbation formulas can be obtained[13] that probably give sufficiently accurate results, but the details of this improved formulation have not been reported. Approximate analytical results are valuable because they help clarify our understanding of the relative importance of the physical phenomena involved. Before relying on approximate formulas that are not supplied with error bounds, however, it is indispensible to check them against results based on less restrictive assumptions, such as those presented here.

In the section on basic physics we shall recall a few essential physical facts relative to the propagation of pulses of incoherent light in optical

fibers. In the section on the characterization of the fiber material, material characteristics, such as the refractive index n and the dispersion $dn/d\lambda_0$, are defined. The numerical integration technique is presented in the section on the evaluation of pulse broadening, with the mathematical derivations relegated to an appendix. This numerical technique is applied to germania-doped fibers in the section on numerical results, and the optimum profiles are calculated. The nature and magnitude of the errors involved in the scalar ray approximation are discussed in the final section. Some of the results reported here have been given previously.[14]

Basic Physics

The physics of optical fibers for communication have been reviewed. See, for example, refs. 13 and 15. We shall recall here a few essential formulas that provide an order of magnitude of the effects considered. In order to evaluate data rates with sufficient accuracy, numerical techniques such as the one discussed in subsequent sections are indispensible.

The transmission capacity of a system (its "bit rate") is determined primarily by the width of the received pulse. It seems reasonable to characterize the received pulse by its root-mean-square width σ, as proposed in ref. 16, where

$$\sigma = \sqrt{<t>^2 - <t^2>} \tag{1a}$$

where, for any quantity a, such as t or t^2, we define

$$<a> = \int_{-\infty}^{+\infty} aP(t)dt \Big/ \int_{-\infty}^{+\infty} P(t)dt \tag{1b}$$

$P(t)$ in Eq. (1b) represents the received optical power P as a function of time. As a rule of thumb, the maximum permissible bit rate can be taken to be $1/4\sigma$. For improved accuracy, one should feed the calculated received pulse $P(t)$ into an error rate computer program. Because, for the kind of power densities usually considered, the fiber material is very nearly linear, and because, for highly multimoded fibers, the usual approximations of space-time ray optics hold, the response of multimode fibers can be assumed to be linear in power. Thus, if one knows the output power $P(t)$ when a brief optical pulse (simulating a δ function) is applied at the input of the fiber, the output power for an arbitrary input pulse follows by convolution.

The two basic causes of pulse broadening in optical fibers are material dispersion and ray (or modal) broadening. The nature of the material dispersion effect is best understood by considering a plane optical wave propagating in a homogeneous medium, perhaps fused silica. The optical wave is assumed to be modulated by a pulse of very small duration, of the order of 100 psec. If the optical source is monochromatic (before modulation) the optical pulse broadening is negligible for all practical purposes. However, some of the most attractive sources presently available have a broad spectral width, much broader than the reciprocal of the pulse duration. For light-emitting diodes in particular, the spectral width is of the order of 4% of the optical carrier frequency. Because the group velocity in the material generally varies with the optical frequency, some frequency components in the pulse arrive ahead of others, causing the pulse to broaden. If $k\ (\omega)$ denotes the slab wavenumber, with $k \equiv (\omega/c)n$, $\omega/c = 2\pi/\lambda_0$, and λ_0 denotes the free-space wavelength, the transit time t of a spectral component at ω is the ratio of the length traveled, L, and the group velocity $u = \partial\omega/\partial k$

$$t(\omega) = \frac{\partial k(\omega)}{\partial \omega} L \tag{2a}$$

Thus, we have

$$t(\omega) - t(\omega_0) \approx \frac{\partial^2 k(\omega_0)}{\partial \omega_0^2} L(\omega - \omega_0) \tag{2b}$$

Within the linear approximation in Eq. (2b), the received pulse $P(t)$ is a replica of the source power spectrum $\mathcal{P}(\omega)$, with scale $dt/d\omega = (\partial^2 k/\partial\omega^2)L$. The above conclusions are based on the assumption of incoherence of the frequency components of the source. Equation (2b) suggests that we define a dimensionless material dispersion parameter

$$M = \frac{\omega^2}{k}\frac{d^2k}{d\omega^2} = \frac{\lambda_0^2}{n}\frac{d^2n}{d\lambda_0^2} \tag{3}$$

For a typical light-emitting diode with a junction at absolute temperature T, the optical spectrum can be approximated by a Gaussian

$$\mathcal{P}(\omega) = \exp\left[-\frac{1}{2}\left(\frac{\hbar\omega - \hbar\omega_0}{KT}\right)^2\right] \tag{4}$$

where $\hbar$ is Planck's constant divided by 2π, K is Boltzmann's constant, and $\hbar\omega_0$ is approximately the band-gap energy. Under the above approximation, the received pulse is Gaussian in shape. If $T = 450°\text{K}$, its rms width is, from Eqs. (2), (3), and (4)

$$\sigma_m\ (\text{nsec/km}) \approx 150 M\lambda_0\ (\mu\text{m}) \tag{5}$$

For fused silica at $\lambda_0 = 0.9\ \mu$m, for example, $M = 0.012$. Thus, accord-

ing to Eq. (5), the rms impulse response width associated with material dispersion is 1.6 nsec/km. The above results are applicable approximately to graded-index fibers, although in general M is a function of dopant concentration and therefore of radius, and some averaging takes place. The averaging effect is particularly important at wavelengths of the order of 1.2 to 1.4 μm, where M may be positive for some dopant concentrations and negative for others. This point will be discussed further later.

Let us discuss ray (or modal) broadening. The carrier is assumed to be monochromatic and modulated by a short pulse that approximates a δ function (quasi-monochromatic short pulse). A multimode source, such as a LED, excites many different rays. The time of flight of the pulse along a particular ray is obtained by integrating along the ray trajectory ds/u, where ds denotes the infinitesimal ray length and $u = \partial\omega/\partial k$, the local group velocity. The refractive index of the cladding sets a lower bound to the axial component of the wavevector (or propagation constant) associated with the rays in the fiber. The dispersion of the cladding material is irrelevant, within the ray approximation. Replacing the cladding material by another one having the same refractive index n_c at the carrier wavelength but a different dispersion $dn_c/d\lambda_0$ may have a considerable effect on the value of $d\Delta/d\lambda_0$, where $\Delta \equiv \Delta n/n$ is the relative change of index in the fiber cross section, but it has no significant influence on the impulse response of the fiber.

It has been shown[3] that for circularly symmetric fibers and quasi-monochromatic sources, the minimum rms impulse response width is independent of dispersion. For the optimum profile, the rms impulse response width is

$$\sigma_d \approx 150\Delta^2 \text{nsec/km} \tag{6}$$

where

$$\Delta = \tfrac{1}{2}\,[1 - (n_{\text{axis}}/n_{\text{cladding}})^2] \approx \Delta n/n \tag{7}$$

For example, if $\Delta = 0.04$, we have, for the optimum profile, $\sigma_d = 0.24$ nsec/km, regardless of the material used. This result has been generalized[17] to a large class of noncircularly symmetric profiles.

In general, the two effects discussed above, material dispersion and ray broadening, combine in a complicated way. For some materials, the quasi-monochromatic impulse response $P(t,\omega)$ merely shifts in time as the optical frequency varies. It is straightforward to show that the rms impulse response width then is

$$\sigma = \sqrt{\sigma_m^2 + \sigma_d^2} \tag{8}$$

where σ_m is given in Eq. (5), and σ_d is given in Eq. (6) for the optimum profile. To solve the general problem one needs to integrate the product $P(t,\omega)\,\mathcal{P}(\omega)$ over ω, where $\mathcal{P}(\omega)$ is the source spectrum. We have

$$P(t) = \int_{-\infty}^{+\infty} P(t,\omega)\mathcal{P}(\omega)d\omega \tag{9}$$

The impulse response $P(t)$ determines the maximum data rate that can be achieved for a given optical power at the receiver and for a specified error rate.

Ideally, the output pulse should be as brief as the input pulse. In fact, some degradation is always suffered. The maximum transmission capacity is reached if (1) we select a light-emitting diode whose peak emission occurs at the wavelength at which $d^2n_0/d\lambda_0^2 = 0$, where n_0 is the fiber refractive index on axis (e.g., $\lambda_0 \approx 1.25$ μm for phosphosilicate fibers) and (2) we select an index profile at λ_0 that minimizes the quasi-monochromatic impulse response at both $\lambda_0 - \Delta\lambda/2$ and $\lambda_0 + \Delta\lambda/2$, where $\Delta\lambda$ denotes the source linewidth. As we have indicated earlier, it is always possible to find an index profile that reduces the quasi-monochromatic impulse rms width, at any given wavelength, down to a value as small as 150 Δ^2nsec/km. To achieve low pulse broadening at two different wavelengths, however, additional degrees of freedom, for example, two dopant materials, are needed.

Characterization of the Fiber Material

In view of the lack of detailed experimental result concerning the anisotropy of fiber materials, we assume in what follows that the ratio n of the free-space wavelength λ_0 and the wavelength λ in the medium is independent of the direction of propagation and of polarization.

We already indicated that to evaluate the broadening of quasi-monochromatic pulses propagating along different rays in optical fibers it is essential to know how the magnitude of the local group velocity u varies with position as well as the variation of the wavenumber k at the carrier frequency considered. Instead of dealing directly with the group velocity, we find it convenient to define a dimensionless dispersion parameter

$$S = -\lambda_0 n(dn/d\lambda_0) \tag{10a}$$

which can be written alternatively

$$S = n^2(D-1) \qquad D \equiv (\omega/k)(dk/d\omega) \equiv v/u \tag{10b}$$

where D is the ratio of the local phase (v) and group (u) velocities. For the materials commonly used in fiber optics, S is of the order of 0.02.

The measured variation of n with λ_0 is usually fitted to a three-term Sellmeier law

$$n^2-1 = \sum_{\gamma=1}^{3} A_\gamma(1-\pi_\gamma)^{-1} \qquad \pi_\gamma = (l_\gamma/\lambda_0)^2 \tag{11}$$

This law involves six coefficients: A_1, A_2, A_3, l_1, l_2, l_3. The parameters l_1, l_2, l_3 physically represent the wavelengths of resonance of the material. Two of them, l_1 and l_2, correspond to ultraviolet resonances, and l_3 is a far-infrared resonance. The physical justification for the Sellmeier law is not important for our present purpose. This law does describe the experimental data accurately. Once the coefficients A_γ, l_γ, $\gamma = 1, 2, 3$ in Eq. (11) have been determined, the dispersion parameter S defined in Eq. (10) can be evaluated at any wavelength from the simple expression

$$S = \sum_{\gamma=1}^{3} A_\gamma\pi_\gamma(1-\pi_\gamma)^{-2} \tag{12}$$

Both n and S vary with the concentration of dopant in the host material, and S can be considered a function of n for any one-parameter class of materials at a given wavelength. The variation of S as a function of n for germania-doped silica, based on measurements made[1] on prisms of bulk samples with the minimum deviation method, is shown in Fig. 1. We have considered two wavelengths of particular interest: $\lambda_0 = 0.9$ μm and $\lambda_0 = 1.06$ μm. The concentration of germania in mole percent is shown near each measured point.

Once we have selected a particular material on axis, it is convenient to introduce, in place of the refractive index $n(r)$ and dispersion parameter $S(r)$, a relative phase index $N(r)$ and a relative group index $\bar{N}(r)$ defined as follows:

$$N(r,\lambda_0) = 1 - n^2(r,\lambda_0)/n_0^2(\lambda_0) \tag{13}$$

$$\bar{N}(r) = [N(r)n_0^2 + S(0) - S(r)]/[n_0^2 + S(0)] \tag{14a}$$

where $n_0(\lambda_0) = n(0,\lambda_0)$ is the refractive index on axis. The dependency on λ_0 is omitted in Eq. (14a) for brevity. $\bar{N}$ can be written alternatively in the form

$$D_\kappa \equiv \bar{N}/N = 1 - \tfrac{1}{2}(\lambda_0/N)(\partial N/\partial\lambda_0)[1-(\lambda_0/n_0)(dn_0/d\lambda_0)]^{-1} \tag{14b}$$

For any given one-parameter class of material, the relative group index

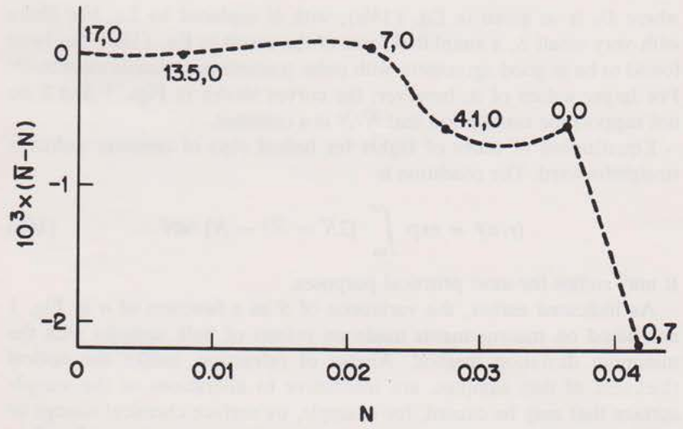

Fig. 2. Variation of the difference $N - \bar{N}$ of the relative group and phase indices as a function of the relative phase index $N \equiv 1 - n^2/n_0^2$ for various materials at a wavelength of $\lambda_0 = 1.06$ μm. The dots correspond to measured points with the concentration of germania and boron oxide in mole percentage shown. The dashed line is interpolated.

$\bar{N}$ can be considered a function of the relative phase index N. This function is obtained from the $S(n)$ curves, such as the ones shown in Fig. 1. A variation of $\bar{N}$ as a function of N is shown in Fig. 2 for a germania- and boron oxide-doped fiber with 17 mole percent germania on axis, at a wavelength of $\lambda_0 = 1.06$ μm.

In the special case in which $\bar{N}/N \equiv D_\kappa$ is a constant within the core,* the optimum profile is very close to a power-law profile.[2,8] The value of the exponent κ of r^2 that minimizes the impulse response width is, exactly[8]

$$D_\kappa/(1+\kappa) = 1/(1+n_c/n_0) \tag{15}$$

where n_c is the cladding refractive index. If, in addition, $\bar{N}/N$ happens to have the same value in the cladding,† the refractive-index profile that minimizes the quasi-monochromatic impulse response width is, exactly

$$N(r) \equiv 1-n^2(r)/n_0^2 = 2\Delta(r/a)^{2[D_\kappa(1+\sqrt{1-2\Delta})\,-\,1]} \tag{16a}$$

* Approximately, this condition means that the index profile does not deform as the wavelength varies (but perhaps does change scale).

† We call "cladding" the region with constant refractive index that usually surrounds the central region (core) with graded index.

where D_κ is as given in Eq. (14b), with N replaced by 2Δ. For fibers with very small Δ, a simplified form of the result in Eq. (16a) has been found to be in good agreement with pulse transmission measurements.[18] For larger values of Δ, however, the curves shown in Figs. 1 and 2 do not support the assumption that $\bar{N}/N$ is a constant.

Equalization of times of flights for helical rays of constant radius is straightforward. The condition is

$$(r/a)^2 = \exp \int_{2\Delta}^{N} [2\bar{N} - \bar{N}^2 - N]^{-1} dN \qquad (16b)$$

It may suffice for most practical purposes.

As indicated earlier, the variations of S as a function of n in Fig. 1 are based on measurements made on prisms of bulk samples with the minimum deviation method. Angles of refraction, unlike the optical thickness of thin samples, are insensitive to alterations of the sample surface that may be caused, for example, by surface chemical change or compacting.[19] Some samples were chilled in order to estimate the effect the rapid cooling that takes place when the fiber is drawn may have on the refractive index (quenching). For germania doping, the effect of chilling is found to be almost negligible. It has a more significant effect on the refractive index of materials such as boron oxide-doped silica. The accidental and systematic errors involved in the measurement of n and $dn/d\lambda_0$ have been estimated. The values given for n appear to be accurate to the fifth decimal place, and the S values given in Fig. 1 to be accurate to within $\pm 1\%$.

Various methods have been proposed to measure the refractive index profile $n(r)$ of fibers directly, including the following:

1. Measurement of the Fresnel reflection from a fresh break of the fiber. (For a recent report and earlier literature see ref. 19.) With deconvolution the resolution afforded by this technique can be as good as $\lambda_0 \sim 1$ μm. Great care must be exercized to avoid chemical or physical degradation of the fiber surface, particularly for boron oxide or phosphor oxide dopants.

2. Measurement of the optical thickness of thin fiber samples with a microscope interferometer. (For recent results, see, for example, ref. 20.) Sample preparation and measurements are very time consuming.

3. Measurement of the intensity in the cross section of the fiber excited by Lambertian sources. (For a recent report, see ref. 21.) Alternatively, a small area of the fiber, of the order of λ_0^2, may be excited with a microscope objective and the total transmitted power measured. (For a theoretical discussion, see ref. 13, p. 257.) This technique is extremely easy to implement. The resolution, of the order of $\lambda/4\sqrt{2\Delta} \approx \lambda_0$, is better than that provided by the interferometric technique. The technique has been applied to fibers with elliptical as well as circularly symmetric profiles, with results reproducible to better than one part in one thousand.[22]

The fine details of a fiber profile can be exhibited by differential chemical etching and observation with an electron microscope, or by electron bombardment and X-ray analysis.

In spite of recent progress, the accuracy and resolution offered by direct measurement techniques do not, at the moment, permit the evaluation of the dispersion curve $S(n)$ with sufficient accuracy. Thus, we have to rely on measurements on bulk samples. Hopefully, the techniques described in 1 and 3 above will eventually prove satisfactory.

Evaluation of Pulse Broadening

Let us first indicate how spatially incoherent sources can be characterized. We select a small portion of the source area with a pin hole, and measure the radiation from that area on a plane screen located at a large distance d from the source. We assume for simplicity that there is an index matching fluid between the fiber and the screen. If $P(x_s, y_s)$ denotes the intensity distribution on the screen, the (unnormalized) source distribution is[13]

$$f(k_x,k_y) = (k/k_z)^4 P\left(\frac{k_x d}{k_z}, \frac{k_y d}{k_z}\right) \qquad k_z^2 = k^2 - k_x^2 - k_y^2 \qquad (17)$$

where k is the wavenumber in the medium between the screen and the fiber. In what follows we assume, for simplicity, that $f(k_x, k_y)$ is a constant when $k_x^2 + k_y^2 \leqq k^2$ and zero when $k_x^2 + k_y^2 > k^2$. Such a source is called "Lambertian." Its radiance is independent of direction. Alternatively, we can say that all the fiber modes that are confined to the source area (including the truncated radiation modes) are equally excited by the source. We also assume that the ray distribution in Eq. (17) and the source spectrum do not vary during the pulse.

Many of the rays excited by the source with different initial positions and slopes differ only by translations along the z axis and rotations about the z axis. Let us call such rays "similar rays." Because the fiber length is always very large compared with the ray periods, pulses that travel on similar rays suffer almost identical delays. It would therefore

be a waste of computer time to evaluate the times of flight of every one of the excited rays (sampled from a continuum) separately. In circularly symmetric fibers, the times of flight depend, in fact, on only two parameters, M and B, where M denotes a normalized axial angular momentum (or aximuthal mode number) and B a normalized axial wavenumber (or propagation constant). The precise definitions of M and B are not needed here (see appendix). The values of M and B are selected from the series

$$M = 1/A, 2/A, \ldots \tag{18}$$

$$B = 2\Delta(I-1)/I, 2\Delta(I-2)/I, \ldots \tag{19}$$

where, as before, $2\Delta \equiv 1 - n_c^2/n_0^2$. Typical values for the constants A and I in Eq. (18) are 50 and 20, respectively. These numbers can be increased for a finer sampling of the rays excited by the source. Strictly speaking, the sequence in Eq. (19) is applicable only to square-law fibers. However, the index profile of large capacity fibers is usually not very different from a square law. While times of flight are extremely sensitive to minute changes of the refractive index profile, the details of the ray sampling procedure are rather unimportant. This is why the approximate sampling series in Eq. (19) can be used.

The time of flight of a pulse along the ray trajectory specified by M and B is obtained by solving with the Euler or Runge-Kutta techniques the system of first-order equations

$$dR/dZ = (1-B)^{-1/2}P \tag{20a}$$

$$dP/dZ = (1-B)^{-1/2}(-\tfrac{1}{2}\, dN/dR + M^2/R^3) \tag{20b}$$

$$dT/dZ = F(R) \tag{20c}$$

where

$$F(R) = (\bar{N}^2 - 2\bar{N} + B)/[1-B + (1-\bar{N})(1-B)^{1/2}] \tag{20d}$$

for the three functions $R(Z)$, $P(Z)$, $T(Z)$, which represent normalized ray radius, ray momentum, and time of flight, respectively. Z is a normalized axial distance. In Eq. (20) N and $\bar{N}$ are assumed to be known functions of the radius r. They were defined earlier in Eqs. (13) and (14), respectively. Within our present scalar ray optics approximation, the impulse response of a fiber is independent of scale, so we can replace r by $R \equiv r/a$, where a denotes an arbitrary length, perhaps the core radius.

The initial values $R(0)$, $P(0)$, and $T(0)$ are defined by

$$R(0) = R_0 \qquad dN(R_0)/dR_0 = 2M^2/R_0^3 \tag{21a}$$

$$P(0) = [B - N(R_0) - M^2/R_0^2]^{1/2} \tag{21b}$$

$$T(0) = 0 \tag{21c}$$

The derivative dN/dR in Eqs. (20) and (21a) can be obtained algebraically if $N(R)$ is given from a simple analytical expression such as a power law or by incrementing R. If the relative refractive index profile is obtained experimentally as a succession of closely spaced points (say, every micrometer radially), the slope dN/dR can be obtained from the values of N at adjacent points. The motivation for using the initial radius R_0 defined in Eq. (21a) is that this radius corresponds to a real trajectory for any permissible value of B at any selected value of M. R_0 depends on M but not on B. The integration of the system in Eq. (20) terminates after one ray period. Usually 1,000 steps per period are enough if the Euler method of integration is used.* The Runge-Kutta method requires fewer steps. The difference between the time of arrival of a pulse along the ray considered and the time of arrival of a pulse along the fiber axis, in nsec/km, is

$$\Delta t = 5{,}000\, T_{\text{final}}/Z_{\text{final}} \tag{22}$$

because the time of flight of axial pulses is approximately 5,000 nsec/km.

The series of values of M and B taken in sequence according to Eqs. (18) and (19) terminates when $P(0)$ in Eq. (21b) ceases to be real, that is, when the quantity inside the square root becomes negative. For a Lambertian source, the rms impulse response width defined in Eq. (1) is obtained by averaging Δt^2 and Δt over all the values of M and B permitted by the condition set up above. The impulse response $P(t,\omega)$ is obtained by counting how many values of M and B correspond to arrival times between t and $t + \Delta t$, where Δt denotes some small time interval.

As ω varies, both the relative index profile $N(R)$ and the dispersion profile $\bar{N}(R)$ usually vary. The impulse response $P(t,\omega)$ needs to be evaluated by the procedure outlined above at various optical angular frequencies ω (or source wavelength λ_0) and summed over ω according

* The Euler method consists of introducing the new values for R, P, Z from the left-hand side of Eq. (20) [e.g., $R_{\text{new}} = R_{\text{old}} + (dR/dZ)\Delta Z$, where ΔZ denotes the integration step] into the right-hand side of these equations. A typical value for ΔZ is $\sqrt{2\Delta}/1{,}000$.

to Eq. (9). If we are interested only in the rms impulse response width, we may use Eq. (1a), where $< >$ is understood now to be a sum over all the rays [sampled by Eqs. (18) and (19)] *and* an integral over all optical frequencies, weighted by the source spectral curve.

Before proceeding with examples, let us summarize the procedure described above. One first measures, with an accuracy better than about 1%, the dispersion parameter $S = -\lambda_0 n(dn/d\lambda_0)$ and the refractive index n for the class of materials considered, for example, silica doped with various amounts of germania. The variation of $\bar{N}$ with N for the class of material considered at some optical angular frequency ω is obtained from these measurements. For an existing fiber, the measured variation of N with radius is fed into the computer program together with the variation of $\bar{N}$ with N to obtain the impulse response $P(t,\omega)$. One then sums $P(t,\omega)$ over the source spectrum, and feeds the result, $P(t)$, into an error rate computer program.

In the procedure described above, we have assumed for simplicity that the slightly leaky rays are totally attenuated and that all the rays suffer the same attenuation. To account for the contribution of the slightly leaky rays to the impulse response the B values in Eq. (19) should be initiated at $2\Delta + M^2$ instead of at 2Δ. For the power transmission of these slightly leaky rays, see, for example, ref. 13, p. 322.

Sometimes the material absorption is not uniform within the core cross section. For example, Rayleigh scattering in germania-doped silica increases with germania concentration. The loss in that case decreases away from axis. The attenuation is obtained, in general, by integrating $k_i ds$ along the ray considered, where k_i denotes the imaginary part of $k \equiv (\omega/c)n$, expressing the local material loss.[13] To account for the nonuniform transmission of the rays, weighting factors need to be introduced in the evaluation of the averages. As is well known, defects in the fiber scatter or couple the modes, and may deeply affect the impulse response. The most recently made fibers, however, exhibit very little mode coupling, so these effects will not be discussed.

To design a multimode fiber, that is, to select the profile $N(R)$ that provides impulse response widths as small as possible for a given class of material, it is convenient to write

$$N(R) = 2\Delta(R^2 + N_2R^4 + N_3R^6 + \ldots)/(1 + N_2 + N_3 + \ldots) \quad (23)$$

and vary the parameters N_2 and $N_3 \ldots$ until the value of σ provided by the computer program appears to be minimum. Usually, optical fiber manufacturers know, at least approximately, how to vary the flow of

dopant during the fabrication of the preform in order to achieve a specified index profile, although successive approximations may be needed.

Numerical Results

The numerical technique described in the previous section has been applied to germania-doped fibers that have a power-law profile at the source wavelength

$$n^2(r) = n^2(0)\,[1-2\Delta(r/a)^{2\kappa}] \quad (24)$$

We used parabolic interpolation-extrapolations from the values of S and n measured at 0, 7, and 13.5 mole percent germania concentration. Two cases were considered: a fiber with 10% germania on axis ($\Delta \approx 0.01$) and a fiber with 20% germania on axis ($\Delta \approx 0.02$). The cladding is assumed to be made of pure silica, and to be unlimited in extent. All propagating modes are assumed to be equally excited and the source is assumed to be quasi-monochromatic. Losses and irregularities are

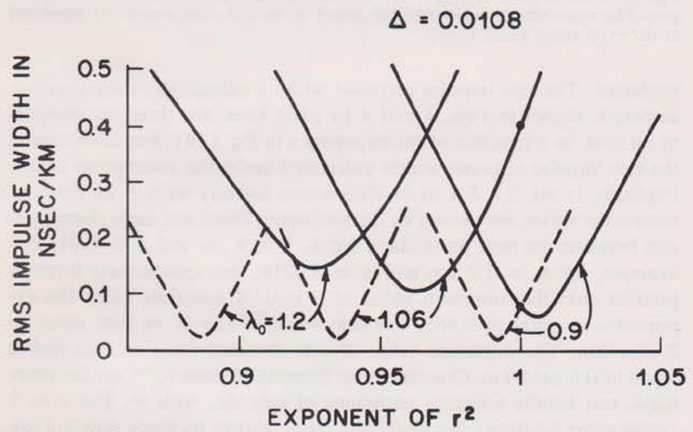

Fig. 3. Variation of the rms impulse response width σ as a function of the exponent κ or r^2 in the power-law profile at the carrier wavelength λ_0 for a germaniadoped fiber. The variation is based on the curves in Fig. 1 and the computer program (solid lines). Approximate results obtained by assuming that $ndn/d\lambda_0$ in Fig. 1 varies linearly with n^2 between the end points are shown by dashed lines. The germania concentration is assumed to be 10 mole percent on axis and zero at the cladding.

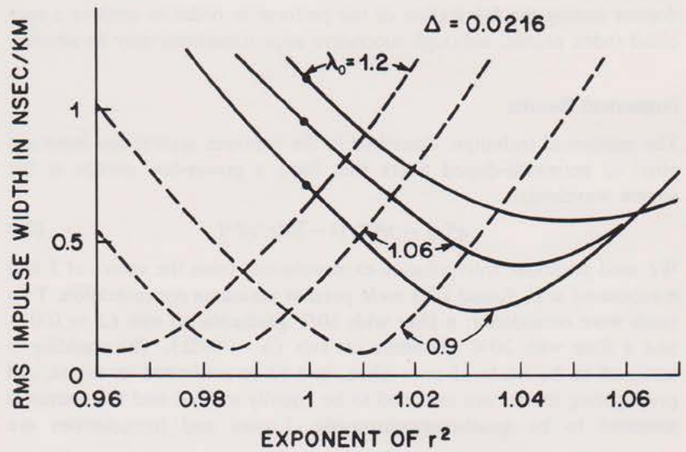

Fig. 4. Continuation of Fig. 3 for 20 mole percent germania concentration on axis. The approximate result (dashed lines) is, in that case, essentially unrelated to the exact result (solid lines).

neglected. The rms impulse response width σ calculated in the previous section is shown in Figs. 3 and 4 by plain lines, for three wavelengths of interest, as a function of the exponent κ in Eq. (24). For comparison, the rms impulse response widths calculated under the assumption (made implicitly in ref. 2) that $n(dn/d\lambda_0)$ varies linearly with n^2 as the concentration varies are shown by dashed lines. There are large discrepancies between the two, particularly for $\lambda_0 > 0.9$ μm and $\Delta > 0.01$. For example, for $\lambda_0 = 1.2$ μm and $\Delta = 0.0216$, the approximate formula predicts that the minimum value of σ is 0.08 nsec/km when the exponent κ is equal to 0.965. For that value of κ, σ is, in fact, equal to 2 nsec/km. The minimum value of σ is obtained for $\kappa = 1.05$ and is equal to 0.6 nsec/km. One analytical formula presented,[12] on the other hand, can handle arbitrary variations of $ndn/d\lambda_0$ with n^2. For $\kappa = 1$ (square-law medium) this analytical result, shown by black dots in Figs. 3 and 4, agrees with the numerical result to better than three decimal places.

Using the form in Eq. (23), the optimum profile for a given class of material has been determined by successive approximations. For example, for a fiber with 17 mole percent germania on axis ($\Delta = 0.022$)

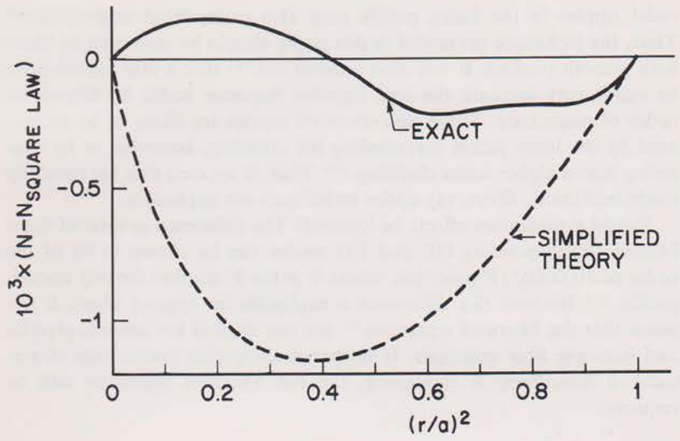

Fig. 5. The solid line represents a correction to the profile (change of relative index with respect to square law) that minimizes pulse broadening. The calculation is based on the curve in Fig. 2. The dashed line corresponds to the optimum profile calculated under the (invalid) assumption that $ndn/d\lambda_0$ varies linearly with n^2.

and $\lambda_0 = 1.06$ μm we find that the rms impulse response width can be reduced to 100 psec/km by a proper selection of the coefficients of the expansion of $n^2(r)$ in series of r^2. This near-optimum profile (solid line in Fig. 5) departs significantly from a power-law profile (dashed line in Fig. 5). The numerical results are in good agreement with the semi-closed form formula[3] and with Eq. (16b).

Wave Optics Effects

The above results rest on the scalar ray optics (or WKB) approximation. In some cases, wave optics effects are significant, even for fibers that have large values of the normalized frequency $V = k_0 a\sqrt{2\Delta}$. In particular, a considerable degradation of transmission capacity takes place when the refractive index profile varies by steps instead of varying smoothly, even when there are as many as 40 steps.[23] Using a first-order perturbation of the Fock parabolic equation (a paraxial form of the scalar Helmholtz equation), it has been shown[24] that small sinus-

oidal ripples in the index profile may also cause large degradation.* Thus, the technique presented in this paper should be restricted to fibers with smooth profiles. It was also pointed out[23] that a few modes close to cutoff may increase the rms impulse response width by almost an order of magnitude. These near-to-cutoff modes are likely to be attenuated by the lossy jacket surrounding the cladding, however, or by tunneling into a higher index cladding.[10] Thus, it appears that for carefully made multimode fibers, ray optics techniques are applicable.

Should polarization effects be ignored? The difference in time of flight between corresponding HE and EH modes can be shown to be of the order of $10{,}000\Delta^2/V$ nsec/km, where V is the V number for any smooth profile.[25] Because this difference is negligible for large-Δ fibers, it appears that the Maxwell equations[7] are not needed for smooth profiles and isotropic fiber materials. If further investigation proves that strain-induced anisotropy is significant, the full Maxwell equations will be required.

Conclusion

The numerical technique presented in this paper is central to the determination of optimum profiles for any large-Δ multimode fiber, and to the evaluation of the effect of arbitrary smooth deviations of the profile from optimum on the transmission capacity. In essence, our technique amounts to integrating three first-order equations over a ray period for different rays excited by the source. Two of these equations provide the ray trajectory for specified initial conditions, and the third equation provides the time of flight of a pulse along the ray trajectory. This numerical technique has been applied to fibers that have a power-law profile at the carrier wavelength but not necessarily at neighboring wavelengths (because of inhomogeneous dispersion). For $\Delta > 0.01$, our numerical results are essentially unrelated to analytical results previously reported.[2] The latter were based implicitly on the assumption that $ndn/d\lambda_0$ varies linearly with n^2 as the concentration varies. Measurements[1] show that this assumption is generally not valid. Using our numerical technique, we have determined approximate optimum profiles for germania- and boron oxide-doped fibers, which follow also from the semiclosed-form result.[3] For quasi-monochromatic sources, profiles can always be found

* With our wave-optics numerical technique we obtained values of σ that agree well (to within 15%) with the first-order perturbation results shown in Fig. 3 of ref. 24.

that reduce the rms impulse response width σ down to about $150\Delta^2$nsec/km. The approximate formula in Eq. (8) suggests that this expression for σ is applicable also to LED sources (that have a nonzero linewidth) if the optical wavelength is properly selected (e.g., $\lambda_0 \approx 1.25$ μm for phosphosilicate fibers). However, the accuracy of Eq. (8) can be questioned. More exact expressions show that, for typical LED linewidths and $\Delta \approx 0.01$, the minimum rms impulse response width is $\sigma \approx 60$ psec/km instead of 15 psec/km.

Detailed and precise comparisons between calculated and measured impulse response are needed before the practical value of the numerical technique presented can be assessed. For the time being, this technique appears to be accurate enough for most multimode fibers. About 1 minute on an IBM 370 computer is required, a much shorter period than that needed by numerical techniques based on the Maxwell equations.

Appendix

Derivation of the Time-of-Flight Equations

The equations that define the time of flight of optical pulses in inhomogeneous anisotropic media are formally simple. They are the Hamiltonian equations

$$d\mathbf{X}/d\sigma = \partial H(\mathbf{K}, \mathbf{X})/\partial \mathbf{K} \tag{A1a}$$

$$d\mathbf{K}/d\sigma = -\partial H(\mathbf{K}, \mathbf{X})/\partial \mathbf{X} \tag{A1b}$$

where $\mathbf{X}$ is a four-vector $\{\mathbf{x}, ict\}$ representing the pulse position $\mathbf{x}$ at time t, and $\mathbf{K}$ is a four-vector $\{\mathbf{k}, i\omega/c\}$ representing the wave vector $\mathbf{k}$ and angular frequency ω of the pulse. $\mathbf{X}$ and $\mathbf{K}$ are considered functions of the parameter σ. At any location $(\mathbf{x})$ and time (t), the properties of the medium are defined by the surface of wave vector

$$H(\mathbf{K}) = 0 \qquad \text{at some } \mathbf{X} \tag{A2}$$

The above formulation appears to be rather abstract. However, once its physical significance has been understood, the specific results needed in fiber optics are easily derived through a succession of straightforward approximations. These transformations have been discussed.[11] We shall therefore omit a few steps and rewrite Eqs. (A1) directly in a form applicable to fibers that are uniform along the z axis and incorporate isotropic lossless materials with wavenumber $k = k(x,y,\omega)$. The arbitrary parameter σ in Eqs. (A1) is now taken to be the axial (z) coordinate.

The five functions $x = x(z)$, $y = y(z)$, $k_x = k_x(z)$, $k_y = k_y(z)$, $t = t(z)$ obey first-order equations

$$dx/dz = k_x/k_z \tag{A3a}$$

$$dy/dz = k_y/k_z \tag{A3b}$$

$$dk_x/dz = (\partial k^2/\partial x)/2k_z \tag{A3c}$$

$$dk_y/dz = (\partial k^2/\partial y)/2k_z \tag{A3d}$$

$$dt/dz = (\partial k^2/\partial \omega)/2k_z \tag{A3e}$$

where

$$k^2(x,y,\omega) = k_x^2 + k_y^2 + k_z^2 \tag{A3f}$$

Physically, k_x, k_y, k_z represent the rectangular components of the wave vector **k**. It is easy to show from Eqs. (A3) that the axial component k_z does not vary along any given ray; k_z is called a constant of motion. Similarly, the optical angular frequency ω is a constant of motion because of the time invariance of the medium. For any given profile $k = k(x,y,\omega)$, the right-hand sides of Eqs. (A3) are explicit functions of x, y, k_x, k_y and of the two constants of motion k_z and ω. If we specify the initial condition on the pulse, namely, its carrier angular frequency ω, the time t at which it intersects the input plane of the fiber, its initial position (x,y), and its slope (related to k_x, k_y), we can evaluate k_z from Eq. (A3f) and proceed with the numerical integration of Eqs. (A3). For noncircularly symmetric profiles, the ray trajectories are usually not periodic. However, the ratio t/z soon tends to a limit as z increases. It is therefore unnecessary to integrate t over the whole length of the fiber.

It is important to observe that Eqs. (A3) are unchanged if x, y, z, and t are multiplied by the same factor, say α. Physically, this means that times of flight per unit length remain the same if we change the scale of the refractive index profile $n(x,y)$. They are the same, for example, for a fiber with a core radius of 40 μm and for a similar fiber with a core radius of 100 μm. The ray periods, however, increase in proportion to α. This scale invariance does not hold when wave optics effects are significant. It is restricted to the ray optics (WKB) approximation.

Let us consider the special case of circularly symmetric fibers with k^2 a function of ω and $r^2 \equiv x^2 + y^2$ only. In that case there is an additional constant of motion, the axial component of the ray angular momentum (or azimuthal mode number)

$$\mu = xk_y - yk_x = rk_\phi \tag{A4}$$

where k_ϕ is the azimuthal component of the wave vector. It is not difficult to show, from Eq. (A3a) to Eq. (A3d), that $d\mu/dz = 0$. The relation (A3f) can now be replaced by

$$k^2 = k_r^2 + k_\phi^2 + k_z^2 \tag{A5}$$

because the r, ϕ, z coordinate system, as well as the xyz coordinate system, is orthogonal. Thus we have

$$k_z = [k^2(r,\omega) - k_r^2 - \mu^2/r^2]^{1/2} \tag{A6}$$

and the Hamiltonian equations are, from straightforward partial differentiation of k_z in Eq. (A6) with respect to k_r, r, and ω, respectively

$$\frac{dr}{dz} = -\frac{\partial k_z}{\partial k_r} = \frac{k_r}{k_z} \tag{A7a}$$

$$\frac{dk_r}{dz} = \frac{\partial k_z}{\partial r} = (\partial k^2/\partial r + 2\mu^2/r^3)/2k_z \tag{A7b}$$

$$\frac{dt}{dz} = \frac{\partial k_z}{\partial \omega} = (\partial k^2/\partial \omega)/2k_z \tag{A7c}$$

The variation of ϕ with z will not be needed.

For any given value of μ, the function $k'(r) = [k_r^2 - \mu^2/r^2]^{1/2}$ can be considered an effective wavenumber, in the sense that it incorporates the effect of the helical motion of the ray, expressed by the term μ^2/r^2. At the turning points of a ray we have $k_r = 0$ and therefore $k' = k_z$. It is clear that the maximum of the curve $k'(r)$ is always located between the two turning points.* It is therefore convenient to choose that particular value of r, say $r = r_0$, as the initial ray radius in the integration of Eqs. (A3). This initial radius r_0 depends on μ (approaching the origin for meridional rays $\mu = 0$), but it is independent of k_z. The initial radius r_0 is thus defined by

$$\partial k'^2(r_0,\omega)/\partial r_0 = \partial k^2(r_0,\omega)/\partial r_0 + 2\mu^2/r_0^3 = 0 \tag{A8}$$

Let us introduce a few convenient transformations. First, according to a previous remark, we can divide r and z by the core radius a without affecting the equations. Thus we set

$$R = r/a \tag{A9a}$$

$$Z = z/a \tag{A9b}$$

* For some ill-behaved refractive index profiles there may be more than two turning points. The ray optics technique presently used is not applicable to such profiles.

Next, we introduce a relative index profile N and a relative wavenumber B

$$N(r) = 1 - k^2(r)/k_0^2 \tag{A10a}$$

$$B = 1 - k_z^2/k_0^2 \tag{A10b}$$

$$k_0 = k(0) \tag{A10c}$$

and set

$$P = k_r/k_0 \tag{A11a}$$

$$M = \mu/(k_0 a) \tag{A11b}$$

in the ray equations (A7a) and (A7b). We readily obtain the ray equation in Eqs. (20a) and (20b) of the main text.

The transformation of Eq. (A7c) giving the time of flight t of a pulse is a little more involved. What we wish to evaluate is the relative time of flight, defined as the ratio τ of the time of flight t of a pulse along a ray to the corresponding time t_0 on axis. The latter is given by

$$dt_0/dz = (\partial k_0^2/\partial\omega)/2k_0 \tag{A12}$$

For computational accuracy, it is advisable to integrate $(t - t_0)/t_0$ rather than t directly.

We now introduce a relative group index $\bar{N}$

$$\bar{N} \equiv [\partial(K_0 N)/\partial\Omega]/(dK_0/d\Omega) \equiv 1 - (\partial K/\partial\Omega)/(dK_0/d\Omega) \tag{A13}$$

where $\Omega \equiv \omega^2$, $K_0 \equiv k_0^2$, $K \equiv k^2$. Equation (A13) can be shown to be equivalent to Eqs. (14). With this notation, we have, from Eqs. (A7c), (A10b), and (A12)

$$\tau - 1 = Z_0^{-1} \int_0^{Z_0} [(1-B)^{-1/2}(1-N)-1]dZ \tag{A14}$$

where Z_0 is the normalized ray period. If dT/dZ is the integrand in Eq. (A14), and we rearrange the terms so that only small quantities appear in the numerator, we obtain

$$dT/dZ = (1-B)^{-1/2}(1-\bar{N})-1 = (\bar{N}^2-2\bar{N}+B)/[1-B+(1-\bar{N})(1-B)^{1/2}] \tag{A15}$$

Equations (20d) and (22) in the main text follow.

References

1. J. W. Fleming, "Measurement of Dispersion in GeO_2-B_2O_3-SiO_2 Glasses," Meeting of the American Ceramics Society, Pocono Manor, Pa. (October 1975).
2. R. Olshansky and D. B. Keck, "Material Effects in Minimizing Pulse Broadening," *Appl. Optics*, **15,** 483 (1976).
3. E. A. J. Marcatili, *Bell System Tech. J.*, **55,** 937 (1976).
4. M. Horiguchi and H. Osanai, "Spectral Losses of Low OH Content Optical Fibers," *Electronics Letters*, **12**, 310 (June 1976).
5. T. P. Pearsall, B. I. Miller, R. J. Capik, and K. J. Bachmann, "Efficient Lattice-Matched Double-Heterostructure LED's at 1.1 μm from $Ga_xIn_{1-x}As_yP_{1-y}$," *Appl. Phys. Letters*, **28**, 499 (May 1, 1976).
6. D. Marcuse, "Microbending Loss of Single Mode Step-Index and Multimode Parabolic-Index Fibers," *Bell System Tech. J.*, **55,** 937 (1976).
7. P. J. B. Clarricoats and K. B. Chan, "Electromagnetic Wave Propagation Along Radially Inhomogeneous Dielectric Cylinders," *Proc. IEE*, **120**, 1371 (1973).
8. J. A. Arnaud, "Pulse Broadening in Multimode Optical Fibers," *Bell System Tech. J.*, **54**, 1179 (September 1975).
9. H. G. Unger, "Optical Waveguides," Conference Proceedings of the Fifth Microwave Conference, Hamburg, Germany (Sept. 1–4, 1975).
10. J. A. Arnaud, "Selection of Waveguide Modes by Two-Dimension Mode Sinks," Digest of Meeting on Integrated Optics, New Orleans, La. (Jan. 21–24, 1974).
11. J. A. Arnaud, "Pulse Broadening in Multimode, Planar, Optical Fibers," *Bell System Tech. J.*, **53**, 1599 (1974).
12. J. A. Arnaud, "Pulse Broadening in Multimode Graded-Index Fibers," *Electronics Letters*, **11,** 8 (Jan. 9, 1975).
13. J. A. Arnaud, *Beam and Fiber Optics* (Academic Press, New York, 1976). Note that the concentrations given in Tables 5.6 and 5.7 are in mole percent. The results for 25% boron oxide correspond to those for a lower concentration of boron oxide (13%). (J. Fleming, private communication.)
14. J. A. Arnaud and J. W. Fleming, "Pulse Broadening in Multimode Optical Fibers with Large $\Delta n/n$ Numerical Results," *Electronics Letters*, **12**, 167 (Apr. 1, 1976).
15. S. E. Miller, E. A. J. Marcatili, and T. Li, "Research Toward Optical-Fiber Transmission Systems. Part I: The Transmission Medium," *Proc. IEEE*, **69**, 1703 (December 1973).
16. S. D. Personick, "Receiver Design for Digital Fiber Optical Communication Systems, I," *Bell System Tech. J.*, **52**, 843 (July–August 1973).
17. J. A. Arnaud, *Electronics Letters*, to be published.
18. L. G. Cohen, G. W. Tasker, W. G. French, and J. R. Simpson, "Pulse Dispersion in Multimode Fibers with Graded B_2O_3-SiO_2 Cores and Uniform B_2O_3-SiO_2 Cladding," *Appl. Phys. Letters*, **28**, 391 (Apr. 1, 1976).
19. J. Stone and H. E. Earl, "Surface Effects and Reflection Refractometry of Optical Fibers," *Opt. Quantum Electronics*, **8,** 459 (1976).
20. D. Gloge, I. Kaminow, and H. Presby, "Profile Dispersion in Multimode Fibers: Measurement and Analysis," *Electronics Letters*, **11,** 469 (Sept. 18, 1975). Note that the basic Eq. (1) of this paper applicable to fibers with inhomogeneous dispersion was given earlier [Eqs. (27) to (29) in ref. 11]. Ref. 11 also shows that this expression reduces to the ray optics results for fibers with large V numbers.

21. F. M. E. Sladen, D. N. Payne, and M. J. Adams, "Determination of Optical Fiber Refractive Index Profiles by a Near-Field Scanning Technique," *Appl. Phys. Letters*, **28**, 255 (Mar. 1, 1975).
22. J. A. Arnaud and R. M. Derosier, to be published.
23. J. A. Arnaud and W. Mammel, "Dispersion in Optical Fibers with Stairlike Refractive Index Profiles," *Electronics Letters*, **12**, 6 (Jan. 8, 1976).
24. R. Olshansky, "Pulse Broadening Caused by Deviations from the Optical Index Profile," *Appl. Opt.*, **15**, 782 (1976).
25. J. A. Arnaud, "Effect of Polarization on Pulse-Broadening in Multimode Graded-Index Optical Fibers," *Electronics Letters*, **11**, 554 (Nov. 13, 1975).